

Supplementary Information for

**Li<sup>+</sup>, Na<sup>+</sup> co-stabilized vanadium oxide nanobelts with bilayer structure for  
boosted Zinc-ion storage performance**

Jinjin Wang,<sup>a</sup> Xiangyuan Zhao,<sup>a</sup> Jinzhao Kang,<sup>a</sup> Xiaomei Wang,<sup>a</sup> Hong Yu,<sup>\*a</sup> Cheng-Feng Du<sup>\*a</sup>  
and Qingyu Yan<sup>b</sup>

<sup>a</sup> *State Key Laboratory of Solidification Processing, Center of Advanced Lubrication and Seal  
Materials, School of Materials Science and Engineering, Northwestern Polytechnical University  
(NPU), Xi'an, Shaanxi 710072, P. R. China*

<sup>b</sup> *School of Materials Science and Engineering, Nanyang Technological University, 50 Nanyang  
Avenue, 639798, Singapore.*

*\* Corresponding Author, E-mail: yh@nwpu.edu.cn, cfdu@nwpu.edu.cn*

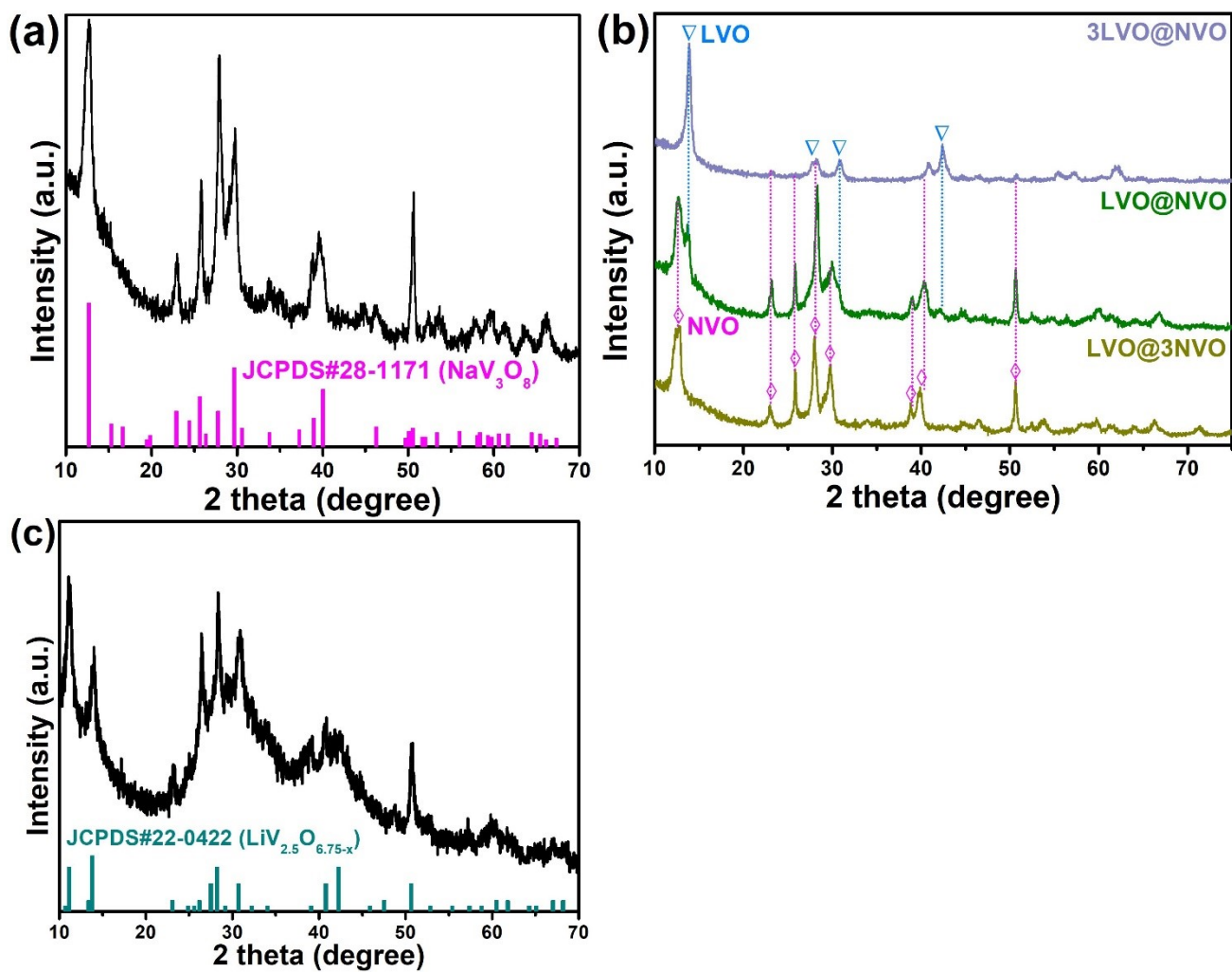


Fig. S1. XRD spectra of (a) NVO, (b) xLVO@yNVO, and (c) the sample prepared with only  $\text{LiNO}_3$ .

Table. S1. The element content of NVO and LVO@NVO materials from ICP-AES measurement.

<b>Materials</b>	<b>Li (wt.%)</b>	<b>Na (wt.%)</b>	<b>V (wt.%)</b>	<b>Ratio</b>
NVO	/	8.33	51.26	Na:V = 1.08:3
LVO@NVO	1.76	3.06	56.25	Li:Na:V = 1.37:0.72:6

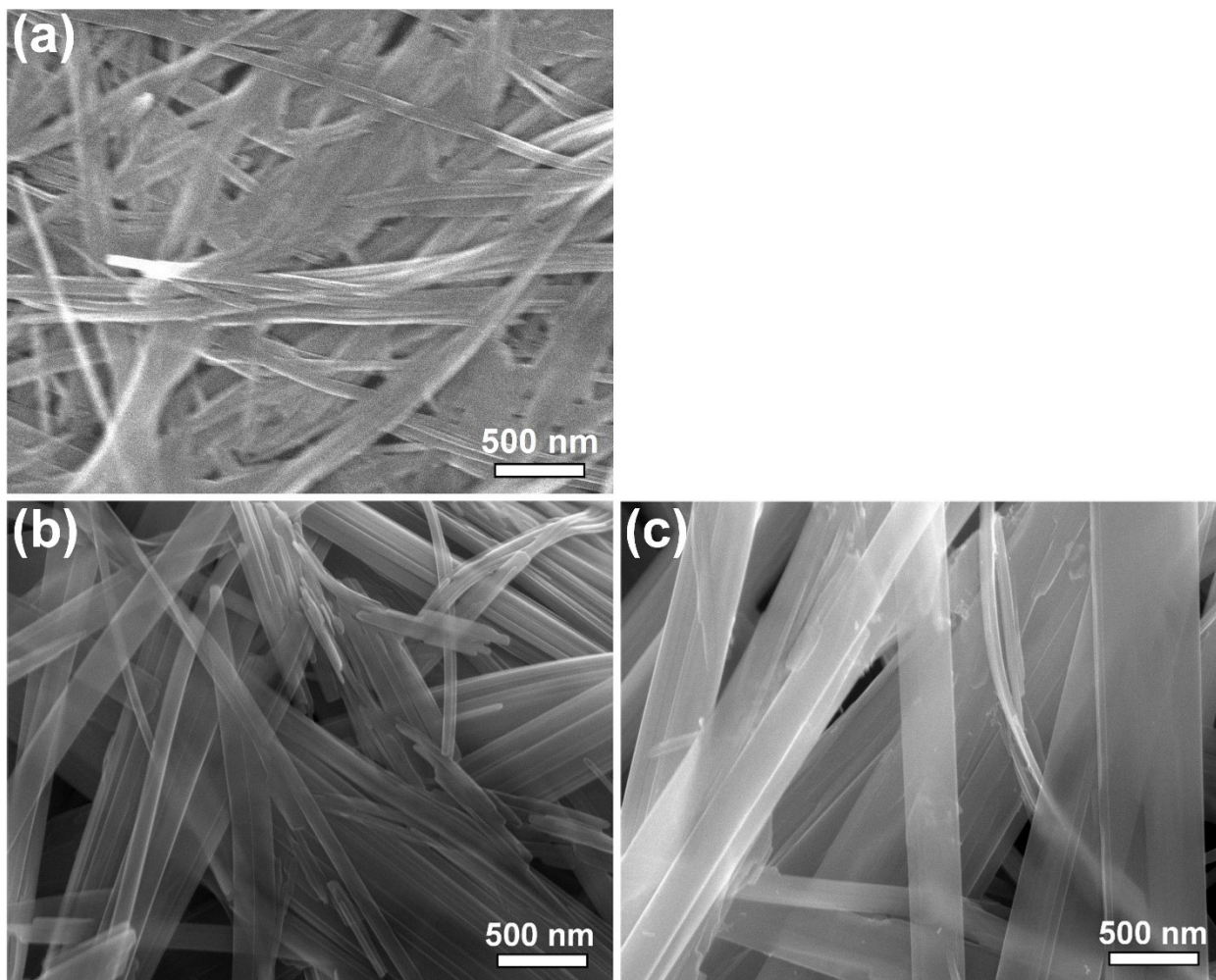


Fig. S2. SEM images of (a) NVO, (b) LVO@3NVO, and (c) 3LVO@NVO.

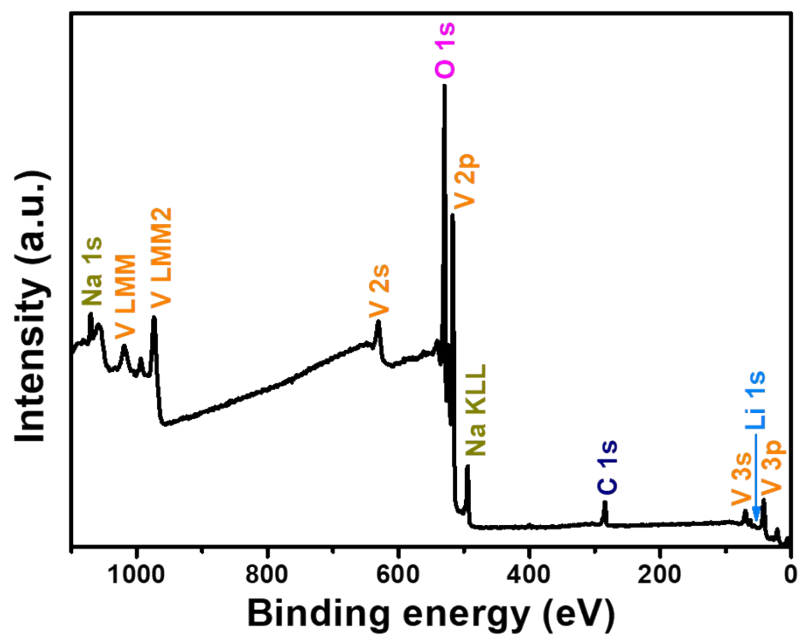


Fig. S3. XPS survey spectrum of the LVO@NVO.

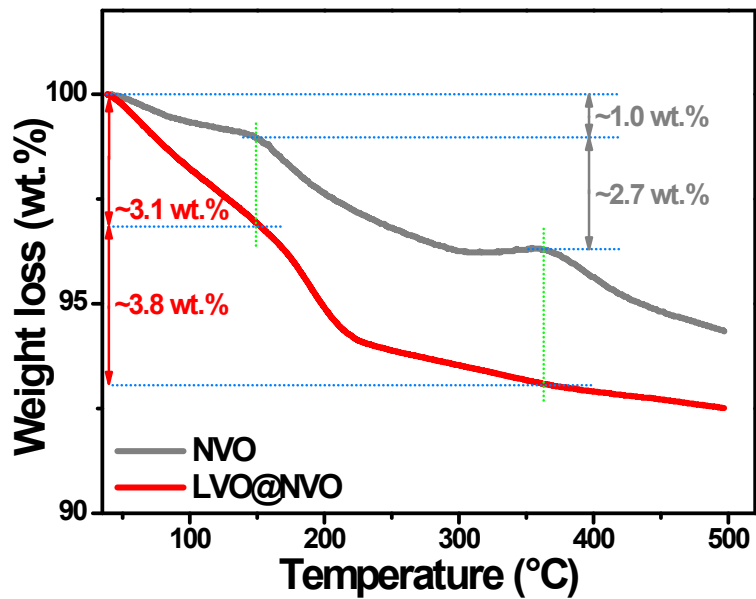


Fig. S4. TGA curves of LVO@NVO and NVO. The weight loss before 150 and 300 °C is related to the removal of free water and structural water, respectively. The free water and structural water are about 3.1 and 3.8 wt.% for LVO@NVO, whereafter 1.0 and 2.7 wt.% for NVO, respectively.

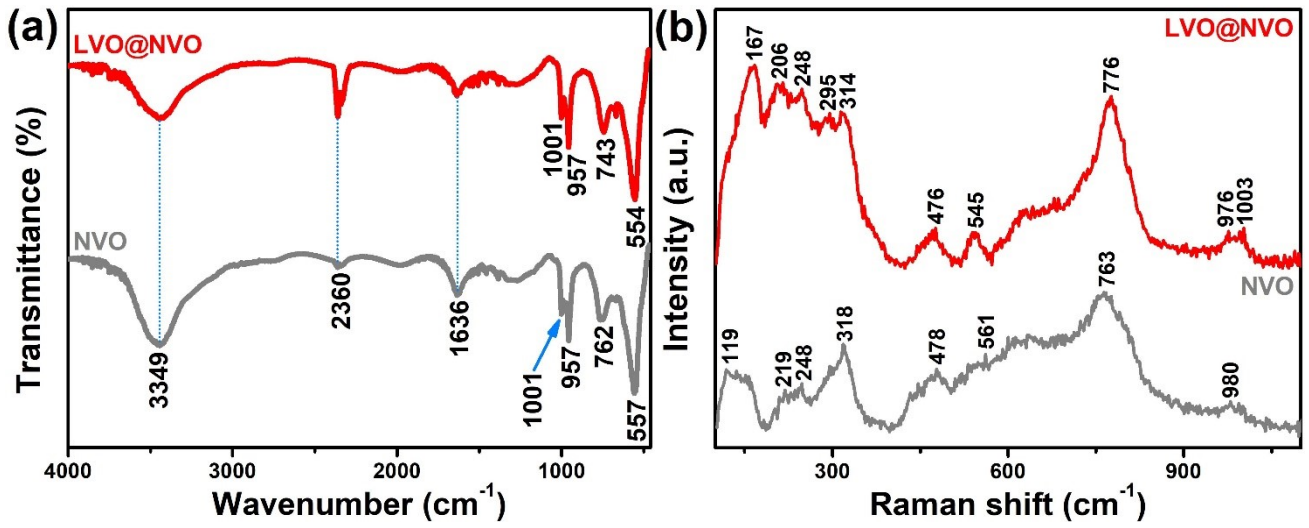


Fig. S5. (a) FTIR spectrum and (b) Raman spectra of the NVO and LVO@NVO.

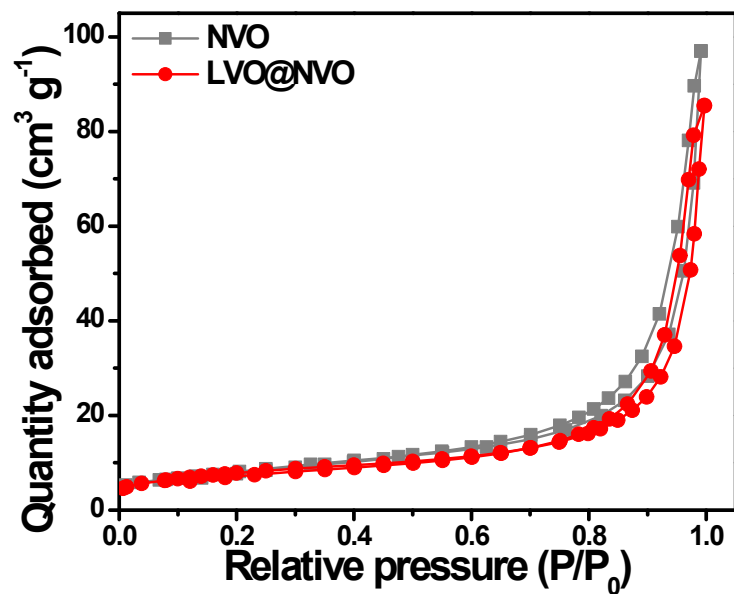


Fig. S6. N<sub>2</sub> adsorption/desorption isotherm of the NVO and LVO@NVO. The BET surface area is 29.33 and 28.16 m<sup>2</sup> g<sup>-1</sup> for NVO and LVO@NVO, respectively.

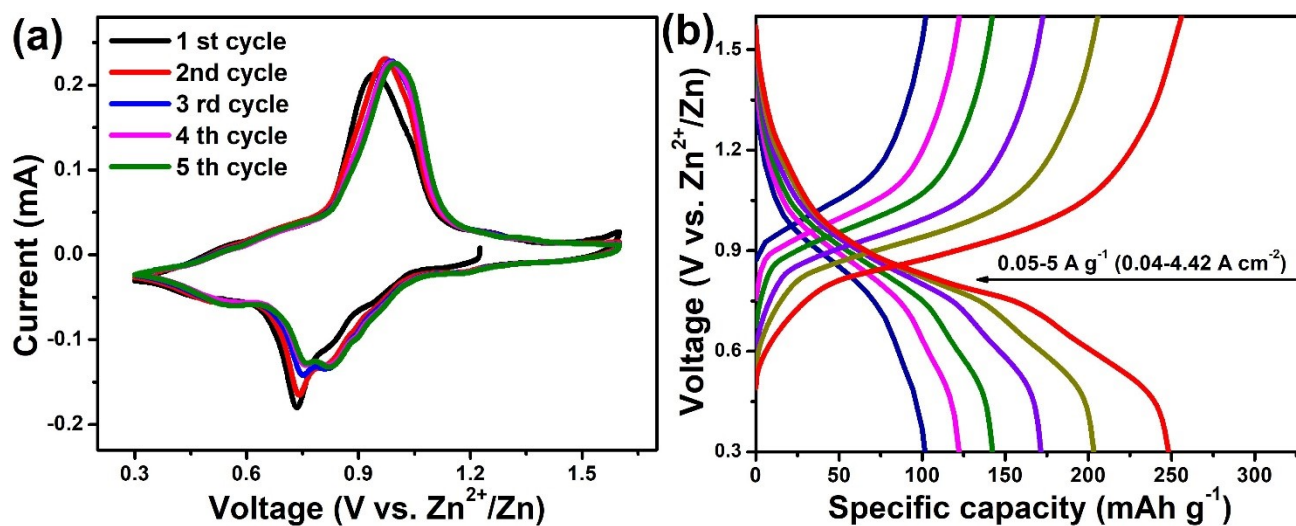


Fig. S7. (a) CV curves and (b) the galvanostatic charge/discharge curves of the NVO cathode.

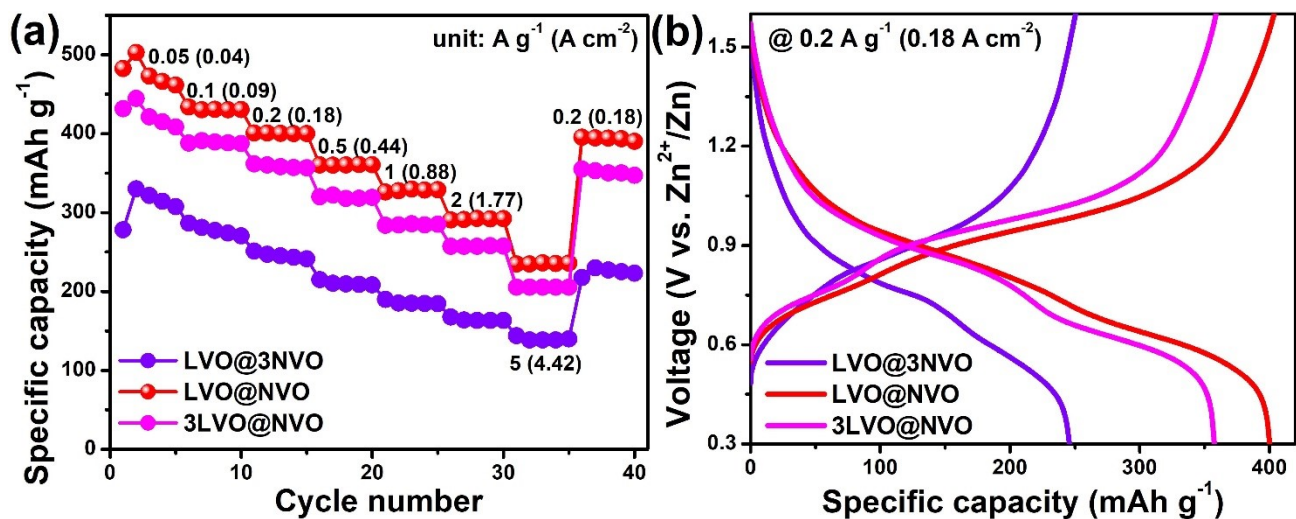


Fig. S8. (a) Rate capacity, and (b) the galvanostatic charge/discharge profiles at the current density of 0.2 A g<sup>-1</sup> for the xLVO@yNVO cathodes.

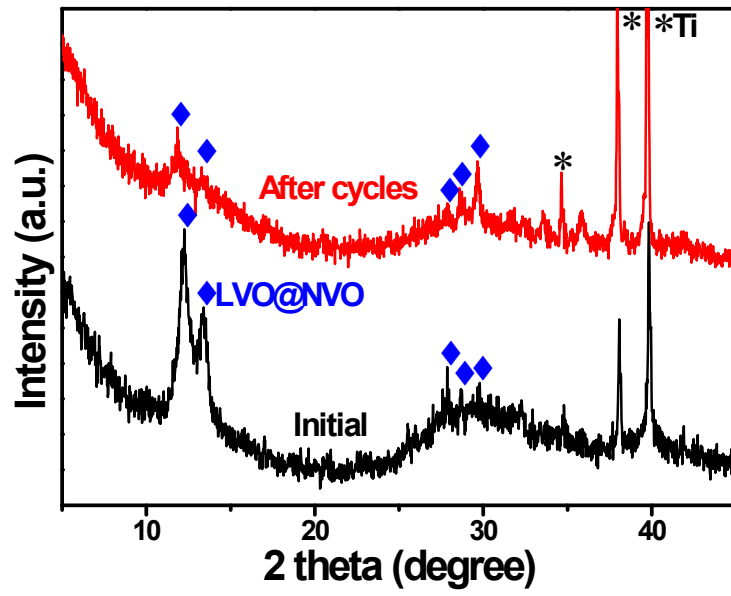


Fig. S9. XRD patterns of LVO@NVO cathodes at initial state and after cycles.

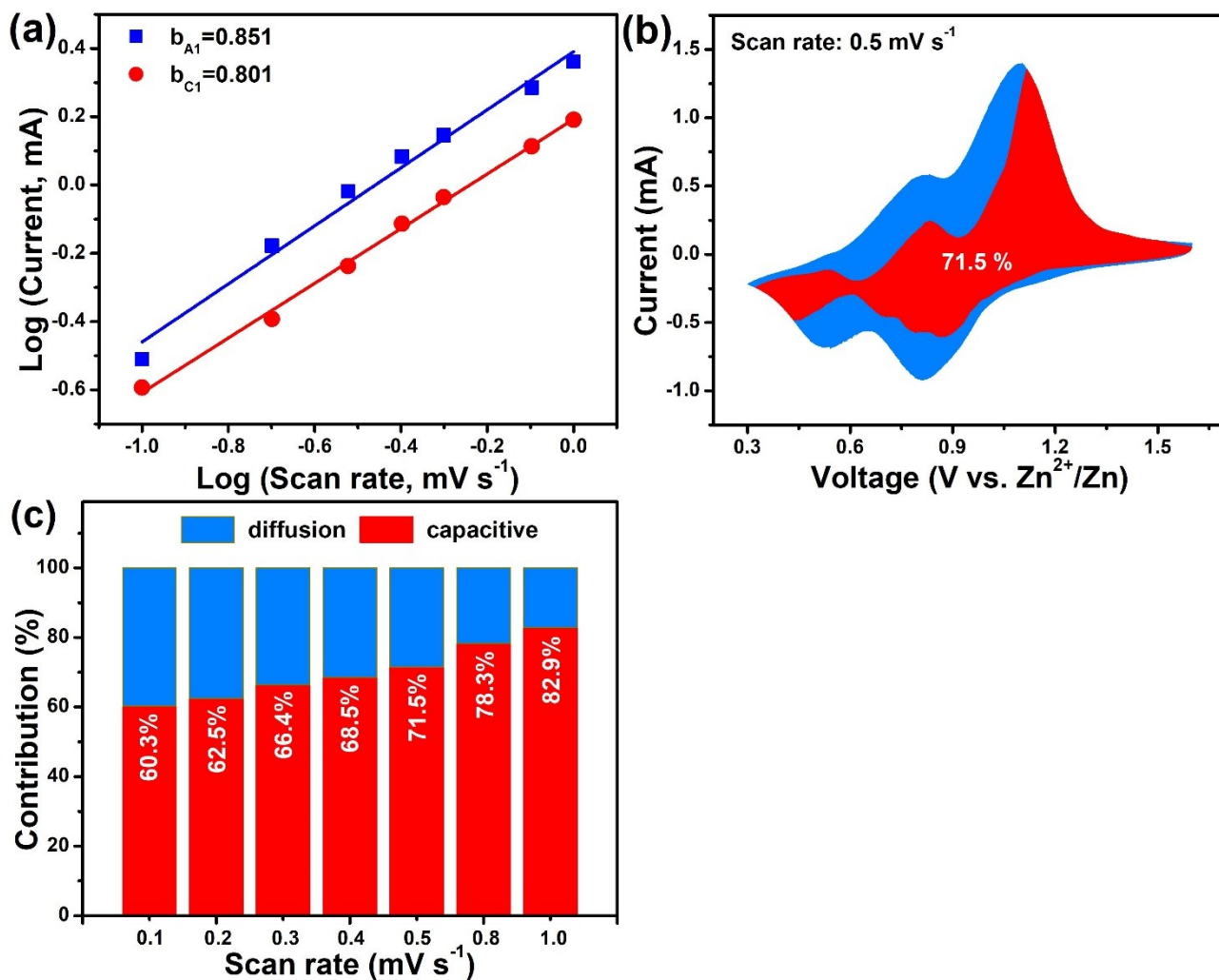


Fig. S10. (a)  $\text{Log}(i)$  vs.  $\text{Log}(v)$ , (b) capacitive contribution (read area) at the scan rate of  $0.5 \text{ mV s}^{-1}$ , and (c) the percentage of diffusion-controlled and capacitive contribution at corresponding scan rates of the LVO@NVO cathode.

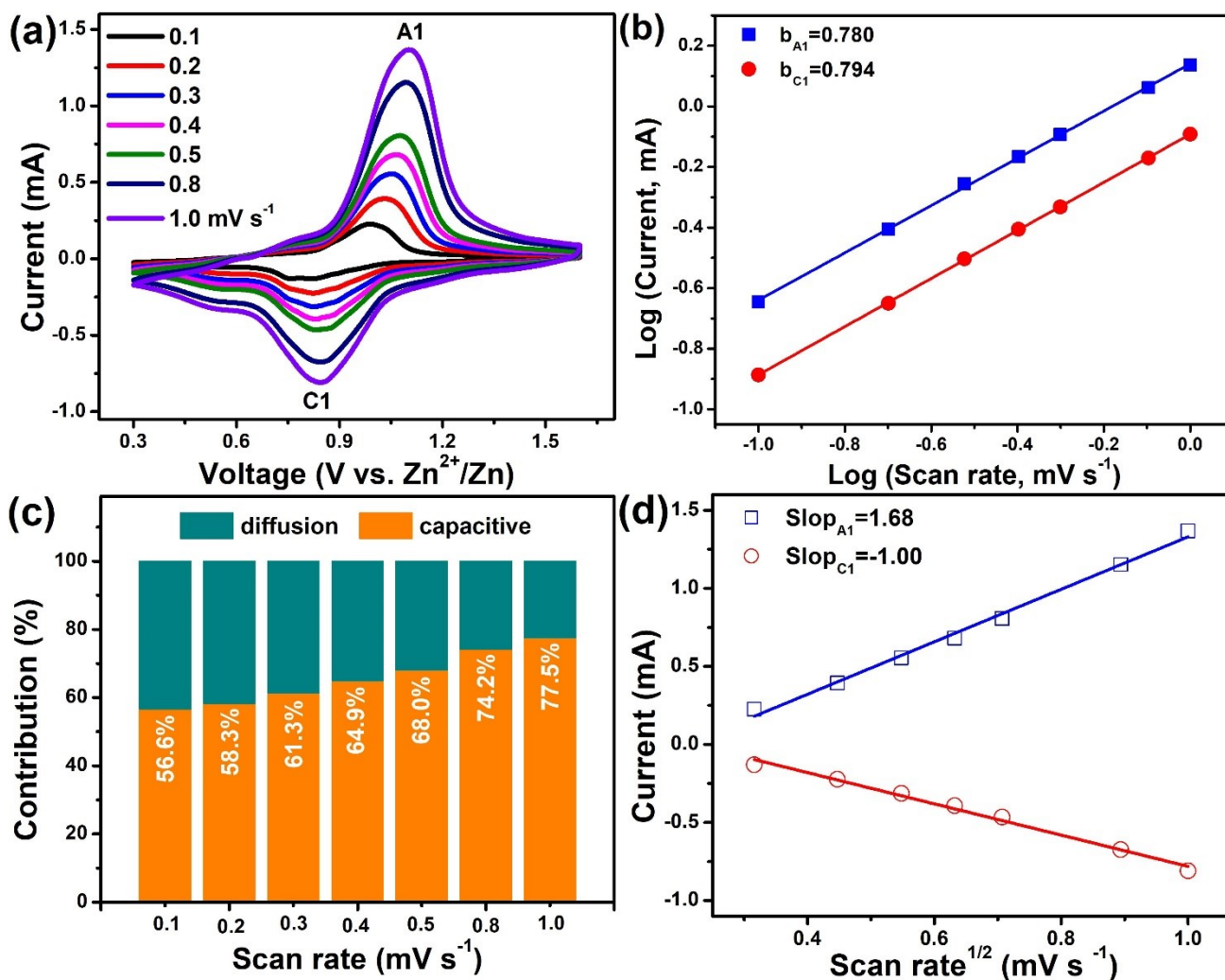


Fig. S11. (a) CV curves, (b) Log  $i$  vs. Log  $v$ , and (c) the percentage of battery-type and capacitance contribution at different scan rates of the NVO cathode. (d) The corresponding linear fitting of the peak current vs. square root of scan rate for NVO.

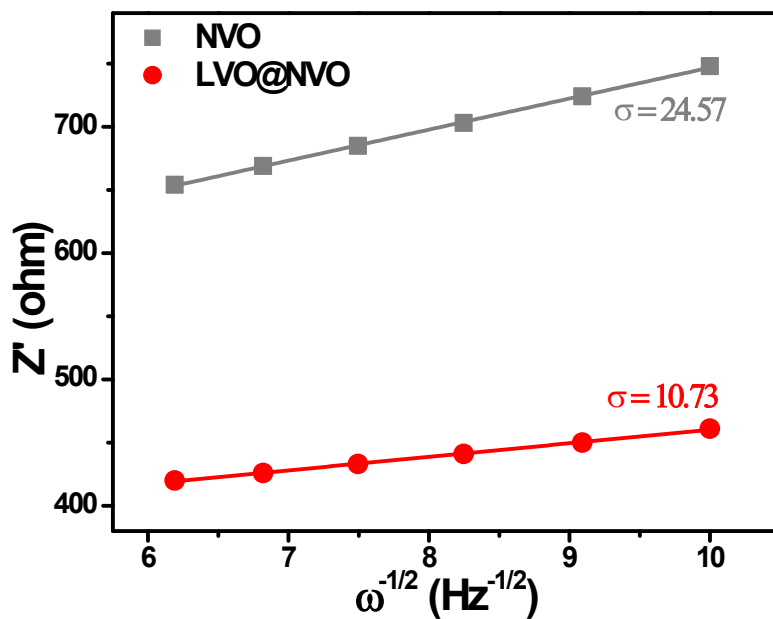


Fig. S12. A linear plot of real resistance ( $Z'$ ) against angular frequencies ( $\omega^{-1/2}$ ) in the low frequency region.

The diffusion coefficient of ions ( $D_{EIS}$ ) is calculated by the following equation:

$$D_{EIS} = \frac{R^2 T^2}{2n^4 F^4 A^2 C^2 \sigma^2}$$

Here,  $R$ ,  $T$ ,  $A$ ,  $C$ ,  $n$ ,  $F$  and  $\sigma$  represent the universal gas constant ( $8.314 \text{ J mol}^{-1} \text{ K}^{-1}$ ), the absolute temperature ( $298 \text{ K}$ ), the valid area of the electrode ( $1.13 \text{ cm}^2$ ), the concentration of ions, the number of electrons, the Faraday constant ( $96485 \text{ C mol}^{-1}$ ), and Warburg coefficient, respectively.

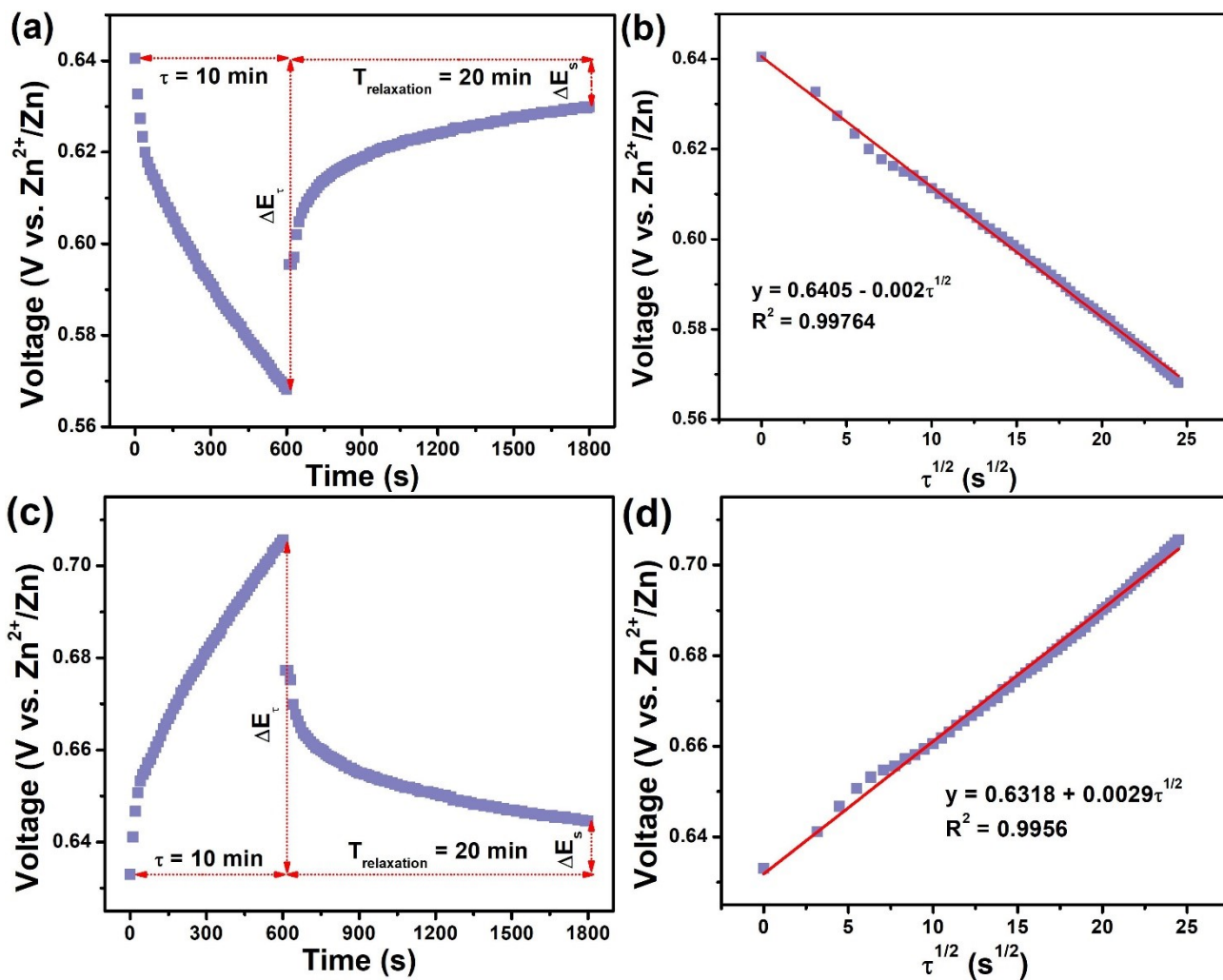


Fig. S13. One single GITT profile of the LVO@NVO cathode in the (a) discharge and (c) charge process. The corresponding linearly fitting behavior for the E versus  $\tau^{1/2}$  in the (b) discharge and (d) charge GITT titration.

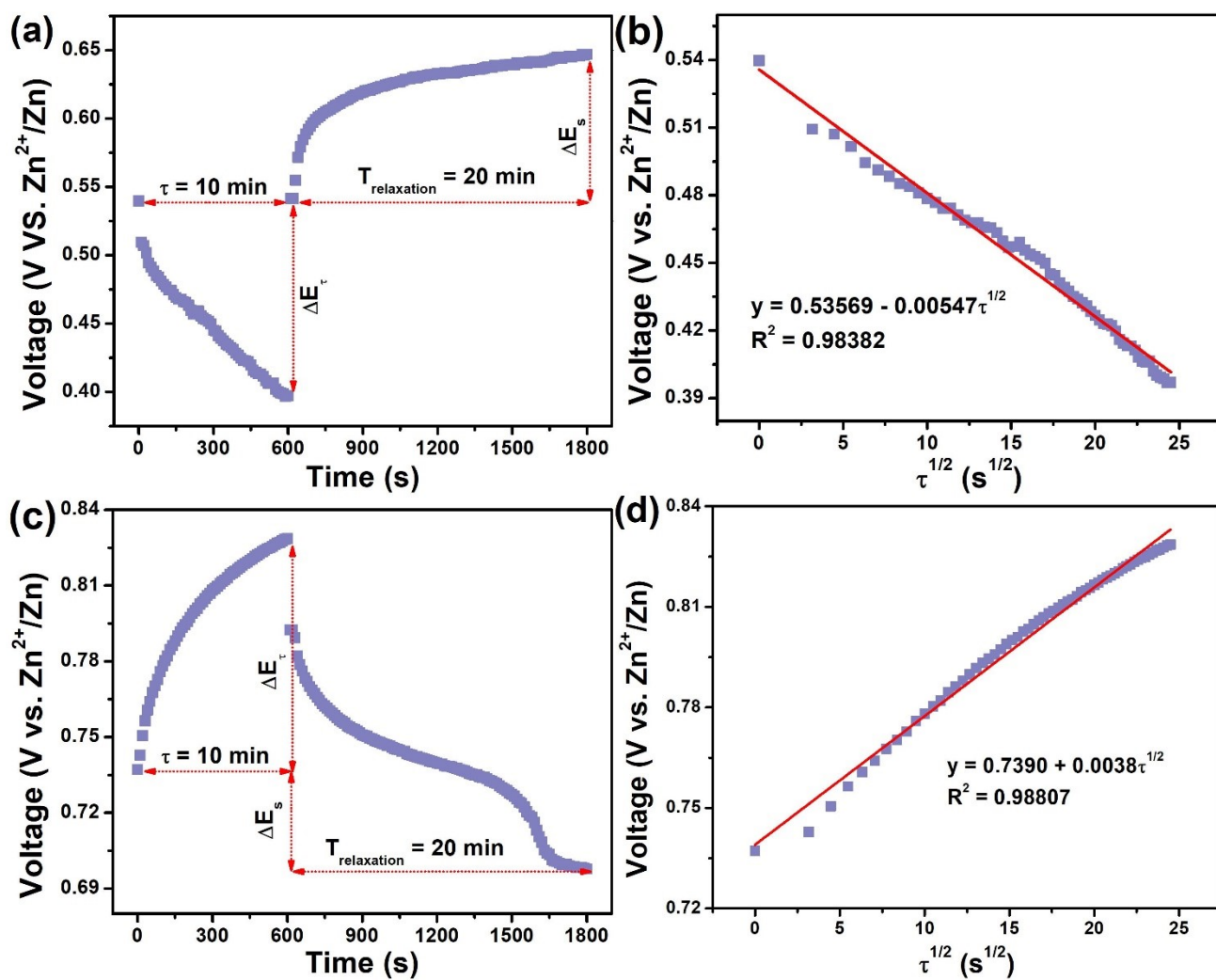


Fig. S14. (a) One single GITT profile of the NVO cathode in the (a) discharge and (c) charge process. The corresponding linearly fitting behavior for the E versus  $\tau^{1/2}$  in the (b) discharge and (d) charge GITT titration.

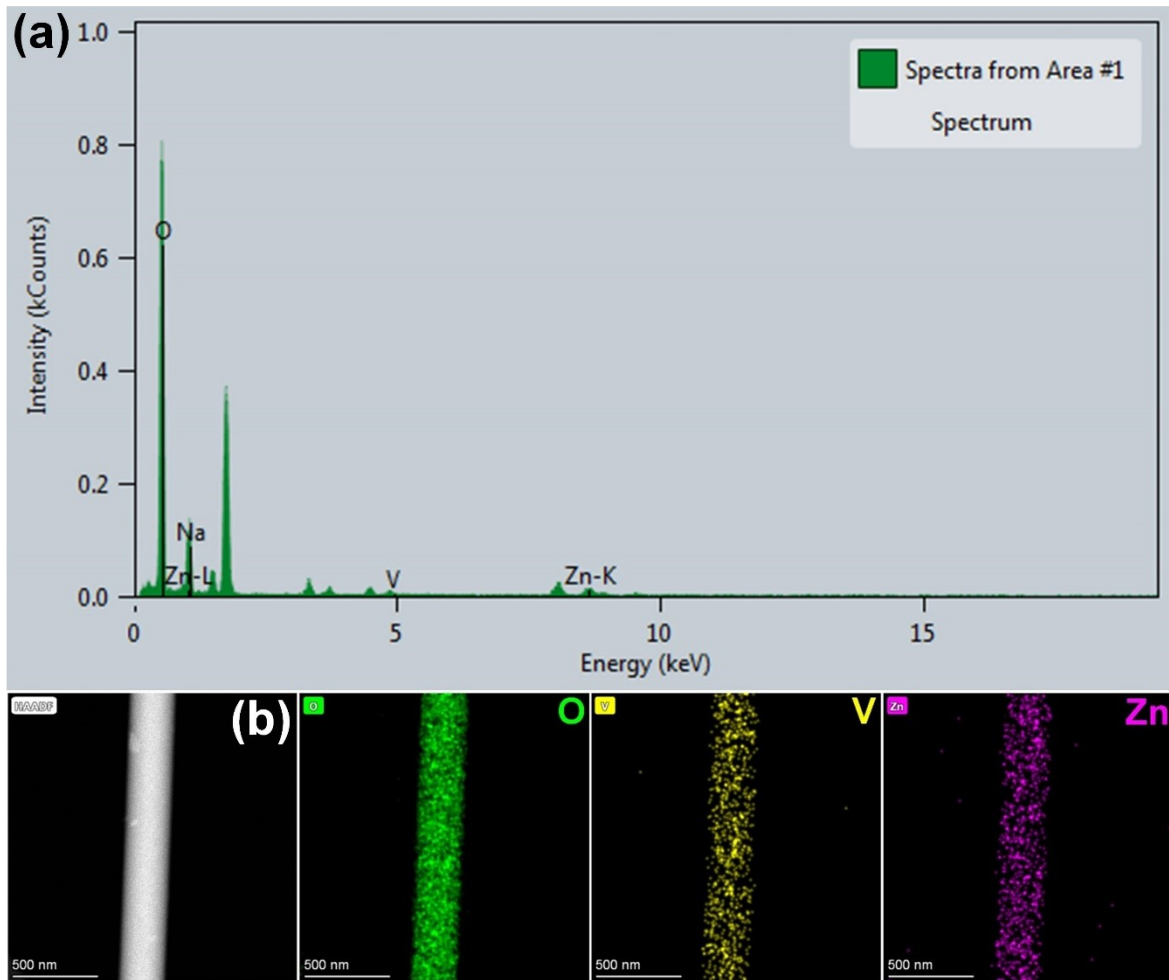


Fig. S15. (a) EDX spectrum, and (b) elemental mapping of the LVO@NVO at D-state.

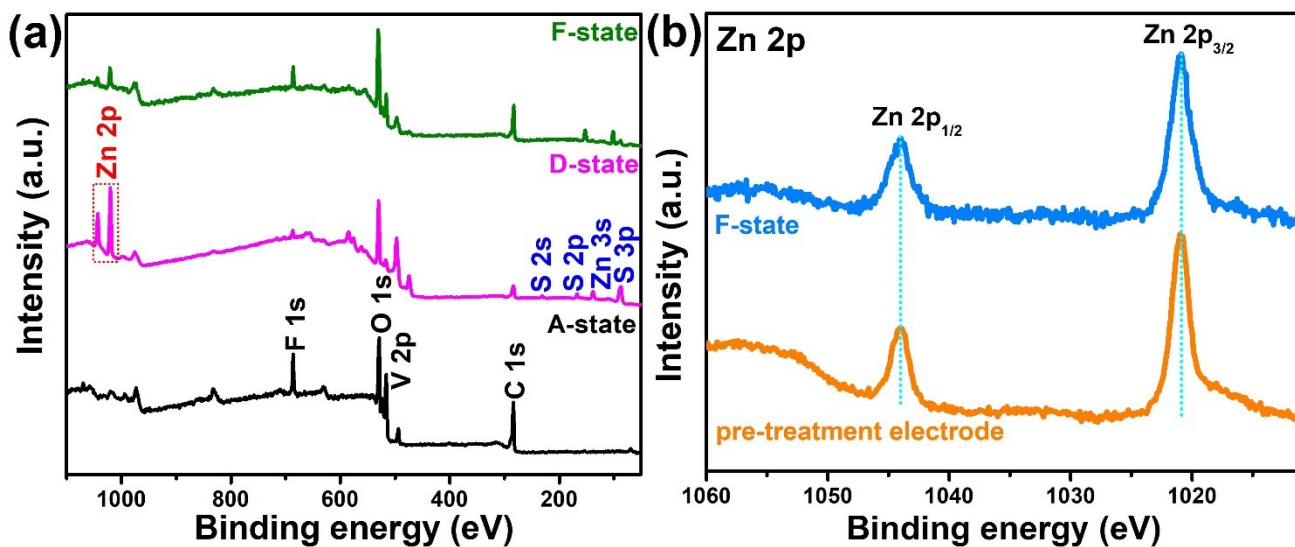


Fig. S16. (a) XPS survey spectrum of the LVO@NVO electrode at the different electrochemical states. (b) Core-level spectra of Zn 2p for different electrodes.